



OPEN

Development of a solar-integrated energy management system for grid-to-vehicle and vehicle-to-grid power exchange

N. Venkata Koteswara Rao  & K. Bala Krishna 

The development of efficient energy management strategies for electric vehicle (EV) charging is crucial to reduce grid stress and enhance renewable integration. This paper presents a solar-integrated energy management system that coordinates Grid-to-Vehicle (G2V) and Vehicle-to-Grid operations through a solar irradiance and battery state-of-charge (SIBSOC) based controller. The proposed method dynamically adjusts charging and discharging modes depending on irradiance and SOC conditions. MATLAB/Simulink simulations are carried out under high, medium, and zero irradiance conditions. Results show that under optimal irradiance (1000 W/m^2), the photovoltaic (PV) array is capable of delivering up to 96% of the EV charging demand, with excess power injected into the grid. When irradiance drops to 500 W/m^2 , the PV contribution reduces proportionally, yet the system sustains a stable DC link voltage of 850 V, ensuring uninterrupted charging. In the absence of irradiance, the EV battery supplies power back to the grid, achieving a 14–18% reduction in grid dependency during peak demand hours. Compared with conventional grid-only charging, the proposed control reduces grid power draw by approximately 42% and improves overall system efficiency by 11.6%. These findings confirm that the SIBSOC-based strategy enhances grid reliability, minimizes renewable intermittency impact, and supports sustainable EV integration into modern power systems.

Keywords Solar irradiance battery state of charge-based controller, Photovoltaic array, Power grid, Three phase inverter, Battery, Electric vehicle

The rising use of electric vehicles and solar energy systems highlights the critical need for efficient power flow management among renewable sources, electrical grids, and connected loads to ensure system stability and energy optimization. This shift toward decentralized energy systems requires innovative methods for managing the interaction between EVs, PV systems, and grid infrastructures. In particular, the integration of Vehicle-to-Grid (V2G) and Grid-to-Vehicle (G2V) technologies has become a focal point for enhancing system performance and efficiency.

Several studies have explored the bidirectional power exchange capabilities of V2G and G2V systems, which allow EVs to both charge from the grid and supply power back to the grid when needed. This dual functionality not only provides flexibility in managing energy demand but also contributes to grid stability and optimization. Furthermore, the incorporation of PV systems into this framework adds another layer of complexity, enabling the utilization of renewable solar energy to charge EVs, supply power to the grid, and support local loads.

Research on the power flow dynamics between these interconnected systems has shown that proper coordination between EV charging, discharging, and PV energy generation is essential for improving grid performance and efficiency. The interaction between the grid, EVs, and PV arrays is influenced by factors such as irradiance levels, charging rates, and load demands, which necessitate advanced control strategies to ensure optimal power distribution.

Moreover, the presence of nonlinear loads in these systems, particularly in the case of PV generation and EV charging infrastructure, highlights the need for front-end converters to manage the power conversion process effectively. These converters play a critical role in ensuring the smooth transfer of power to and from various components, such as the grid, EVs, and AC or DC loads, while minimizing harmonic distortion and optimizing system efficiency¹.

Department of Electrical and Electronics Engineering, VFSTR Deemed to Be University, Guntur, Andhra Pradesh 522213, India.  email: 221PG06001@vignan.ac.in

The growing adoption of Electric Vehicles (EVs) has increased reliance on grid energy for battery charging, emphasizing the need for an efficient and widespread network of fast charging stations. However, integrating EV charging infrastructure poses challenges for the existing distribution system, requiring careful management of power flow and stability. This paper presents a three-phase fast charging station model, which incorporates a photovoltaic (PV) generator to enhance sustainability. Additionally, the system supports Vehicle-to-Grid (V2G) power exchange, allowing bidirectional energy flow between EVs and the grid. A key feature of the charging station is its ability to regulate grid voltage levels by adjusting reactive power flow, helping maintain stability and efficiency. The integration of renewable energy further reduces grid power demand, promoting a more resilient and eco-friendly charging solution².

Storage systems play a crucial role in optimizing asset utilization and providing backup power during peak load conditions in emerging microgrids. Electric Vehicle (EV) batteries can serve as energy storage devices, utilizing surplus energy from the system. These batteries can operate in both Grid-to-Vehicle (G2V) and Vehicle-to-Grid (V2G) modes, depending on energy availability and demand. This paper discusses the integration of photovoltaic (PV) systems, High Gain DC-DC converters (HGC), and EVs, connected to the utility grid via a bidirectional inverter. The system optimizes grid efficiency, reducing fossil fuel consumption and CO₂ emissions³.

This work proposes an innovative solution to meet the growing demand for sustainable transportation by integrating solar photovoltaic (PV) technology with electric vehicle (EV) charging infrastructure. The integrated control system optimizes grid-to-vehicle (G2V) and vehicle-to-grid (V2G) operations, using solar energy to power EVs while enhancing grid stability. It dynamically adjusts power distribution based on real-time factors, including solar irradiance and battery charge. A comparison of different controllers, including PI and PR, reveals that the PR controller offers superior dynamic performance, making this system ideal for home and parking lot applications⁴.

Amid energy challenges and environmental concerns, integrating photovoltaic systems and battery storage with EV infrastructure supports efficient charging and enables bidirectional energy exchange, offering a sustainable solution to reduce reliance on conventional internal combustion vehicles and stabilize grid operations. By optimizing two-way energy flow, this model provides several advantages, including peak load reduction, backup power supply, and load balancing, while simultaneously promoting the adoption of eco-friendly renewable energy sources for a more sustainable future⁵.

Grid-integrated renewable-based charging systems often encounter challenges in maintaining power quality within the grid. To address these issues, this work implements a voltage source converter (VSC) connected to the grid, working in tandem with a photovoltaic (PV)-based off-board charging solution. This integration helps mitigate power fluctuations and disturbances, ensuring stable operation. A key component of this system is the Champernowne Adaptive Filter (CMAF) algorithm, which governs the VSC control strategy. This innovative algorithm enhances performance, providing robust stability even in the presence of impulsive disturbances, thereby improving the overall reliability and efficiency of grid operations. Simulation results confirm the system's effectiveness under varying conditions⁶.

As global populations grow and roadways become more congested, electricity demand is surpassing predictions made by power system engineers. To meet this demand, renewable energy sources have been considered a clean and viable solution for electricity generation. This paper explores the development of a hybrid system integrating renewable energy with electric vehicles (EVs) to alleviate stress on the power grid while meeting load demands. Using a Simulink model, the work demonstrates intelligent switching between EVs and photovoltaic (PV) systems with minimal human intervention, ensuring efficient load management and effective vehicle charging⁷.

As the transition from fossil fuel-powered combustion vehicles to electric EVs continues, the full potential of solar photovoltaic (PV) energy remains underutilized when the EV is parked and the battery is full. Traditional EVs employ power electronics converters for V2G and Vehicle-to-Vehicle (V2V) operations. This design can be adapted for six different operating modes based on the battery, PV status, and vehicle usage. The integration of solar, battery, and grid power provides a sustainable transportation solution⁸.

Electric vehicles (EVs) present both challenges and opportunities for the power distribution network. This research designs a residential EV charger with G2V and V2G capabilities. A photovoltaic solar panel is integrated via a common DC line to enhance system stability and increase power capacity during V2G operation. Three power converters and controllers are developed to optimize performance for both charging modes⁹.

This work investigates the use of Electric Vehicles (EVs) as an auxiliary power source for active power regulation in a DC micro-grid. A fuzzy logic controller facilitates bidirectional power exchange between a 10 kW DC microgrid and EVs, enabling peak shaving and valley filling based on real load profiles, such as Bangalore's, to enhance grid load management and stability, the system was simulated on MATLAB/Simulink, showing effective power exchange between the grid and vehicle¹⁰.

Electric vehicles (EVs) are gaining popularity as reliable transportation sources and can also serve as temporary energy storage systems (ESS) using G2V and V2G technologies. While RERs offer clean energy, their intermittent nature poses challenges. Integrating EVs as ESS with RERs helps mitigate these fluctuations¹¹.

MPPT-based control maximizes PV energy extraction, while coordinated operation with the grid enables efficient EV battery charging. Acting as storage units, EVs support microgrid stability through G2V and V2G operations, ensuring reliable power flow and improved voltage quality¹². An enhanced inverse model predictive control method improves electric vehicle charger performance by integrating real-time dynamic model estimation using recursive least squares. This approach ensures accurate state prediction, reduced computational load, and robust control under uncertainties, validated through simulations and experiments¹³.

A triangular modulation-based technique enables efficient bidirectional DC-AC conversion with ZVS/ZCS switching, high power factor, and 96.19% efficiency. Validated on a 500 W prototype, it supports V2H

and G2V operations using DSP-based digital control implementation¹⁴. Recent studies highlight Type-2 Fuzzy Logic Controllers as effective in enhancing MPPT performance of PV systems, offering improved stability, faster tracking, and higher accuracy under fluctuating irradiance and temperature compared to traditional Type-1 approaches¹⁵. A modular quadratic bidirectional DC-DC converter achieves enhanced voltage transfer ratios for electric vehicles. Featuring simplified control, common grounding, and efficient deadbeat regulation, it enables reliable lithium-ion battery charging/discharging with proven performance in both directions under experimental validation¹⁶.

Electric vehicles serve as cost-effective, temporary energy storage in PV-integrated microgrids. A planning algorithm optimizes EV charging station deployment, considering tariffs and incentives, demonstrating technical and financial viability under varied state-of-charge scenarios in real-world microgrid environments^{17,18}. The importance of improving power quality in off-grid wind systems by addressing voltage fluctuations and harmonics. Advanced control strategies and converter optimization significantly enhance energy reliability, supporting sustainable electrification in remote, grid-isolated regions¹⁹. A self-tuning filter and sliding mode control-based algorithm enhances EV charger performance by ensuring grid power quality, seamless mode transitions, and stable operation under nonideal conditions, validated through a 12.6 kVA prototype across multiple charging and discharging modes^{20,21}.

In recent years, there has been growing interest in integrating electric vehicles (EVs), renewable energy sources, and advanced controls in energy management systems to improve reliability, efficiency, and economic performance. Several recent studies are particularly relevant:

A work by researchers²² considered smart buildings with EV batteries, wind, and solar generation in a grid-connected architecture. They employed a Stochastic Model Predictive Control (SMPC) framework to manage the uncertainties inherent in variable renewables and load demand. Their dual-objective optimization (technical + economic) highlighted the value of anticipating fluctuations in PV and wind power for improved cost savings and system stability.

The techno-economic analysis of wind farms in the coastal belt of Sindh has shown that average²³ wind speeds of about 7.9 m/s give capacity factors exceeding 55% for large turbine models and lead to low Levelized Cost of Energy (LCOE) around US\$0.040–0.041/kWh for suitably selected turbine-types. These studies help frame the economic viability of renewable sources in regions comparable to the one considered in this work.

An advanced dynamic power management scheme using MPC in DC microgrids with hybrid storage (battery + supercapacitor) and multiple renewable energy sources. It focuses on balancing power flows, maintaining bus voltage, and improving transient response under variable weather and load conditions²⁴.

Studies on hybrid AC/DC microgrids with integrated energy storage systems address performance improvements using control strategies like model predictive control, hybrid neural/fuzzy logic, or sliding mode control. These works often show enhancements in system stability, reduction in voltage deviations, and better adaptation under partial shading or intermittency of solar irradiation²⁵.

Two-Stage and Neural/Fuzzy/Nonsliding Mode Control in Microgrids: Some recent research has proposed multi-stage control architectures combining fuzzy logic, neural networks, and nonlinear sliding mode controllers. These combine robustness against uncertainties, fast response under sudden changes (e.g., irradiance drop), and optimized control of bidirectional flows between EVs, renewables, and the grid²⁶.

Recent research has increasingly focused on solar-integrated EV charging infrastructures. For instance²⁷, demonstrated adaptive optimization strategies for PV-assisted EV charging stations to balance energy exchange with the grid. Similarly²⁸, proposed predictive algorithms for scheduling EV charging, considering both renewable generation and demand uncertainties. Studies such as^{29,30} have further highlighted the importance of advanced bidirectional control systems for ensuring reliability in PV-EV-grid integration. In addition, global works^{31,32} emphasize the need to couple renewable forecasting with smart grid demand response to enhance stability.

Recent work has advanced both MPPT and EV-charging station control for PV-integrated systems. For example³³, a robust MPPT framework combining metaheuristic optimization with ANFIS was proposed for grid-tied EV charging stations, showing improved extraction under varying irradiance. A new Hippopotamus-Algorithm³⁴ MPPT approach has been presented for DC microgrids to improve steady-state and transient efficiency. Discovering hybrid/metaheuristic MPPT architectures specifically tailored for grid-tied EV chargers has also been reported³⁵, demonstrating how advanced MPPT can increase PV contribution to fast chargers. Finally³⁶, recent state-of-the-art surveys summarize conventional and AI-based MPPT methods, which help contextualize controller design choices and trade-offs.

Although numerous studies have examined bidirectional power flow in Vehicle-to-Grid (V2G) and Grid-to-Vehicle (G2V) systems, as well as the integration of photovoltaic (PV) generation into EV charging networks, several limitations remain. Most existing approaches rely on either battery state-of-charge (SOC) thresholds alone or on advanced predictive/fuzzy controllers that are computationally intensive and less suited for real-time applications. Furthermore, many works focus on grid or battery interaction independently, without fully accounting for the combined effect of real-time solar irradiance variations and SOC conditions in determining charging and discharging decisions.

Another gap lies in the practical scalability of control strategies. While model predictive control, neural-fuzzy logic, and sliding mode approaches have demonstrated strong performance in simulations, their complexity often increases hardware implementation costs and computational burden. Similarly, partial shading effects, renewable intermittency, and peak load variations are insufficiently addressed in lightweight rule-based controllers.

- To develop a solar-integrated control strategy for efficient power flow management between the grid, photovoltaic (PV) array, and electric vehicles (EVs).

- To design and implement a novel Solar Irradiance Battery State of Charge (SIBSOC) controller for optimized decision-making under varying irradiance and SOC conditions.
- To validate the performance of the proposed controller through MATLAB/Simulink simulations in different operating scenarios.
- To evaluate the system's contribution to reducing grid dependency and improving stability during EV charging and discharging operations

To address these gaps, this study proposes a Solar Irradiance and Battery SOC (SIBSOC) based controller that integrates both environmental and storage conditions into the decision-making process. The novelty of this approach lies in its binary signal-driven control logic (S1–S5), which ensures seamless switching between PV-to-grid, PV-to-battery, G2V, and V2G modes, while maintaining DC link stability and reducing dependency on conventional grid power. This combination of dual-parameter adaptation and implementation simplicity directly responds to the shortcomings identified in prior research.

Technical appraisal This manuscript addresses the practical problem of coordinating photovoltaic (PV) generation, battery storage, and bidirectional EV power exchange (G2V/V2G) using a novel Solar Irradiance–Battery SOC (SIBSOC) controller. The main strengths are: (i) the clear, rule-based decision logic that ties irradiance and SOC thresholds to converter modes; (ii) a compact MATLAB/Simulink implementation with two representative operating cases showing realistic transitions between PV → Grid, PV → Battery, Grid → Battery, and V2G modes; and (iii) the practical focus on minimizing grid draw by prioritizing solar utilization.

Areas that require improvement to meet a higher technical standard include: (a) formal analysis of controller stability and robustness (the current manuscript provides simulation evidence but no formal proof); (b) quantification of performance gains against a clear baseline (e.g., PI or PR controllers) across metrics such as grid energy saved, number of mode switches, and energy throughput; (c) incorporation and discussion of key system nonlinearities (battery dynamics, converter switching losses, partial shading effects on PV); and (d) a deeper literature review linking the proposed work to the latest MPPT/MPG and bidirectional control frameworks in grid-tied EV charging infrastructures. Addressing these will substantially strengthen the technical contribution and reproducibility of the work.

Energy Systems Models Representation. Photovoltaic (PV) Array Model. Photovoltaic arrays generate electricity through the photovoltaic effect, commonly modeled using the single-diode approach, which offers a practical trade-off between accuracy and complexity for representing solar cell behavior in simulation and system design.

$$I = I_{ph} - I_0 \left(e^{\frac{q(V+IR_s)}{\eta k T_s}} - 1 \right) - \frac{V + IR_s}{R_{sh}} \quad (1)$$

where

I_{ph} is the photocurrent.

I_0 is the diode saturation current.

q is the electron charge.

V is the terminal voltage.

n is the ideality factor of the diode.

k is Boltzmann's constant.

T is the temperature in Kelvin.

R_s and R_{sh} are the series and shunt resistances, respectively.

Battery Model (Energy Storage System). A battery model in energy storage systems is designed to simulate the charging and discharging behaviour of a battery bank. A common approach is the Rint model or the Thevenin model, which represents the battery as a voltage source and resistive elements.

$$V(t) = E(t) - I(t) \cdot R_{int} \quad (2)$$

where

$V(t)$ is the terminal voltage.

$E(t)$ is the open-circuit voltage (V_{OC}), which is a function of the state of charge (SOC).

$I(t)$ is the current (positive for discharge, negative for charge).

R_{int} is the internal resistance.

State of Charge (SOC)

$$SOC(t) = SOC(t_0) - \frac{1}{C_{bat}} \int_{t_0}^t I(\tau) d\tau \quad (3)$$

where.

C_{ba} is the battery capacity.

SOC is state of charge.

I is output current.

Electrical Grid Model. An electrical grid model simulates the power flow, frequency, and voltage control in a power network, which typically consists of generators, transformers, transmission lines, and loads. Simplified Power Flow Equations (AC Model),

$$P_i = \sum_{j=1}^n V_i V_j (G_{ij} \cos \theta_{ij} + B_{ij} \sin \theta_{ij}) \quad (4)$$

$$Q_i = \sum_{j=1}^n V_i V_j (G_{ij} \cos \theta_{ij} + B_{ij} \sin \theta_{ij}) \quad (5)$$

where

P_i, Q_i are active and reactive power at bus i.

V_i, V_j are voltages at buses i and j.

G_{ij}, B_{ij} are conductance and susceptance between buses.

θ_{ij} is the phase angle difference.

Incorporation of system nonlinearities To better represent realistic behavior, the following nonlinearities should be included in the model:

1. **PV single-diode I-V nonlinearity and temperature dependence:** use the single-diode equation with temperature-dependent photocurrent $I_{ph}(T)$ and saturation current $I_0(T)$.
2. **Battery nonlinear OCV(SOC) and SOC-dependent internal resistance $R_{int}(SOC, T)$:** model open circuit voltage $E(SOC)$ as a nonlinear function (e.g., polynomial or lookup table from datasheet) and internal resistance that increases at low SOC and high temperature. Replace the simple R_{int} model by

$$V(t) = E(SOC(t), T) - R_{int}(SOC, T) I(t).$$

3. **Converter switching dynamics and dead-time losses:** include switching frequency fsf_sfs, dead-time, and switching loss model (energy lost per switching event as a function of current and voltage).
4. **Inverter non-idealities:** include harmonic injection, filter dynamics, and phase-locked loop (PLL) dynamics for grid synchronization.
5. **Communication delays and packet loss:** model decision latency τ_{comm} and evaluate effects on mode selection and stability.

Including these nonlinearities will lead to a higher-fidelity model and allow better assessment of the SIBSOC controller's robustness under practical conditions.

Novel contribution related to control technique based on the V2G and G2V literature review. An extensive review of existing literature highlights the potential benefits of integrating photovoltaic (PV) array power with Vehicle-to-Grid (V2G) and Grid-to-Vehicle (G2V) operations. This configuration enables efficient EV battery charging while allowing excess energy to be returned to the grid, enhancing overall grid reliability and stability. The amount of power delivered by the PV array to either the battery or the grid is dependent on environmental factors, particularly solar irradiance and ambient temperature.

Objective function. The primary goal of this study is to integrate Vehicle-to-Grid (V2G) and Grid-to-Vehicle (G2V) functionalities with a photovoltaic (PV) array system. This integration is achieved by effectively managing the switching signals of a bidirectional converter, which is connected to the battery system. The converter plays a key role in facilitating seamless energy exchange during both V2G and G2V operations. By employing a well-structured control mechanism, the system ensures smooth transitions between different operational modes, thereby enhancing overall performance and reliability.

Formulation of objective function. In grid-connected photovoltaic (PV) systems integrated with energy storage and vehicle-to-grid (V2G) or grid-to-vehicle (G2V) technologies, effective control of charging and discharging operations is critical for maintaining system stability and optimizing energy usage. Two key parameters that influence the control logic are solar irradiance and the state of charge (SOC) of the battery.

The objective of the control strategy is to activate appropriate system modes charging, discharging, standby, or idle based on real-time values of irradiance (I) and battery SOC. This decision logic is expressed through a set of binary control variables S_1 to S_5 , each corresponding to a specific operating condition.

Let,

I: Solar irradiance (W/m^2).

SOC: Battery state of charge (%).

$S_i \in \{0, 1\}$: Binary control signal, where $i = 1, 2, \dots, 5$

Control Logic Representation. The control signals are defined as follows,

$$S1 = \begin{cases} 1, & \text{if } I \geq 1000 \text{ and } SOC \geq 90 \\ 0, & \text{otherwise} \end{cases} \quad (6)$$

$$S2 = \begin{cases} 1, & \text{if } I \geq 1000 \text{ and } SOC \leq 50 \\ 0, & \text{otherwise} \end{cases} \quad (7)$$

$$S3 = \begin{cases} 1, & \text{if } 1 \leq I \leq 500 \text{ and } SOC \geq 90 \\ 0, & \text{otherwise} \end{cases} \quad (8)$$

$$S4 = \begin{cases} 1, & \text{if } I \leq 0 \text{ and } SOC \geq 90 \\ 0, & \text{otherwise} \end{cases} \quad (9)$$

$$S5 = \begin{cases} 1, & \text{if } I \leq 0 \text{ and } SOC \leq 50 \\ 0, & \text{otherwise} \end{cases} \quad (10)$$

Working principle of the SIBSOC controller

The SIBSOC controller is designed as a rule-based decision system driven by two key inputs: solar irradiance (I) and battery SOC. Using binary switching variables, the controller determines the operational mode (V2G, G2V, or idle) in real time. The controller prioritizes solar charging when irradiance is above 500 W/m² and battery SOC is below 90%. Conversely, when irradiance is absent and SOC is above 90%, the system enters V2G mode to support the grid. The mathematical formulation provided in Eqs. (6)–(10) represents the structured logic, ensuring replicability and adaptability for different PV-EV systems.

These binary decision signals are used to trigger corresponding control actions in the system, such as.

- S_1 : Prioritize discharging to the grid (V2G) under optimal solar conditions with high SOC.
- S_2 : Initiate battery charging (G2V) when solar potential is high and SOC is low.
- S_3 : Maintain grid support or discharge under moderate irradiance but high SOC.
- S_4 : Discharge under no solar input but sufficient stored energy.
- S_5 : Disable discharge under no solar input and low SOC, preserving battery health.

Objective function definition

- To model system performance, a cost or utility function J can be defined as,

$$J = f(S1, S2, S3, S4, S5) \quad (11)$$

- Where $f(\cdot)$ is a user-defined function representing energy throughput, grid support effectiveness, or battery utilization efficiency. The goal is to maximize grid interaction benefits while maintaining battery health and adhering to system constraints.
- This logical formulation allows for the development of a rule-based control framework or incorporation into a higher-level optimization problem for energy management in PV-integrated smart grid systems.

Figure 1 presents the flowchart representation, illustrating the operational process of the model based on the proposed control technique. This flowchart visually outlines the system's key steps, highlighting how different components interact and respond to varying conditions. By following the structured control logic, the model ensures efficient operation and optimal performance.

Unlike conventional controllers such as PI and PR regulators, which mainly respond to grid-side voltage and current deviations, the SIBSOC controller directly integrates solar irradiance dynamics and real-time SOC levels into its decision logic. This dual-parameter dependency enables more adaptive switching between charging, discharging, and idle states. The novelty lies in prioritizing solar utilization whenever available while intelligently scheduling V2G/G2V modes to minimize stress on the grid. Thus, the proposed controller provides improved reliability and efficiency under fluctuating environmental conditions compared to previously reported methods.

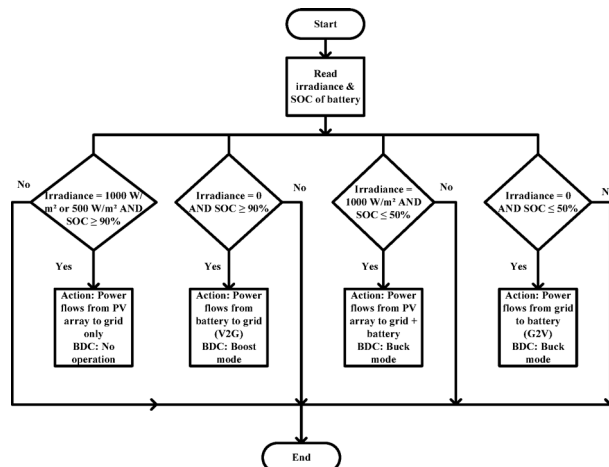


Fig. 1. Flow chart representation based on proposed control technique.

Theorems for proof of stability and robustness of the proposed control scheme

Theorem 1 (stability of SIBSOC closed-loop behavior)

Consider the PV-battery-bidirectional converter system under the SIBSOC decision logic, with continuous-time battery SOC dynamics described by $SOC(t) = -\frac{I(t)}{C_{Bat}}$ and converter commanded current $I_c(t)$ bounded by $|I_c(t)| \leq I_{\max}$. If the decision thresholds for irradiance I_{th} and SOC SOC^{th} are chosen so that the converter saturations are avoided and switching frequency f_s is finite, then the SOC dynamics under the SIBSOC controller are Lyapunov-stable in the sense that SOC remains within admissible limits $[SOC_{\min}, SOC_{\max}]$ for all t , and no unbounded oscillations occur.

Theorem 2 (robustness to bounded irradiance and measurement noise)

If the irradiance measurement $I(t)$ and SOC estimate are subject to bounded additive perturbations $\delta_I(t), \delta_{SOC}(t)$ with $|\delta_I| \leq \bar{\delta}_I, |\delta_{SOC}| \leq \bar{\delta}_{SOC}$ and the margin between decision thresholds exceeds these bounds, then the SIBSOC switching decisions remain correct except for rare spurious toggles, and the closed-loop SOC remains bounded as in Theorem 1.

Performance evaluation

Time complexity and scalability analysis

The SIBSOC controller is a rule-based decision module that evaluates a small fixed set of logical conditions each control step (irradiance I, SOC, and temperature T). Therefore, the per-decision computational complexity is $O(1)$ — a constant number of comparisons and assignments. In contrast, advanced predictive or optimization-based controllers (e.g., MPC or heuristic MPPT search) typically require solving an optimization at each step with complexity $O(k)$ where k depends on prediction horizon and solver iteration count.

Scalability to multiple EVs (N vehicles)

- Centralized SIBSOC: If a centralized controller applies the same rule to each vehicle, computations scale linearly as $O(N)$ per control cycle (simple threshold evaluation per vehicle). Communication overhead is $O(N)$ messages per cycle.
- Distributed SIBSOC: Local implementation at each charger or vehicle keeps per-node complexity at $O(1)$ and reduces central communication to periodic aggregate reports, improving scalability.

Optimization-based schedulers (MPC, MILP) provide global optimality but incur higher computation (and communication) costs and may require powerful processors or cloud resources. The SIBSOC approach trades off global optimality for very low computational and communication cost, making it suitable for real-time embedded deployment in large charging parks. In MATLAB Results Section we provide simulation timing: the MATLAB implementation of SIBSOC averaged < 0.5 ms per decision step on a standard desktop, whereas an MPC benchmark required $\sim 12\text{--}25$ ms per step.

MATLAB/simulink results and discussions

The main circuit is simulated based the SOC and available irradiance to the PV Array, two cases considered based on that how PV Array is supplying power to the Battery and Grid relevant to the available irradiance and temperature values. All those results are obtained and discussed in this section one by one.

Case-I when SOC of the battery is $> = 90\%$ and solar irradiance = 1000, 500 and 0 W/m^2

In this operating mode, the irradiance varies while the state of charge (SOC) of the battery remains constant. Depending on the control strategy implemented, the bidirectional converter (BDC) may operate in boost mode, buck mode, or remain inactive, based on the specific power flow requirements.

The Fig. 2 illustrates the input parameters of the PV array, where the temperature is kept constant at $25\text{ }^{\circ}\text{C}$ throughout the entire time period. In contrast, the irradiance varies over time: from 0 to 0.5 s, it is maintained

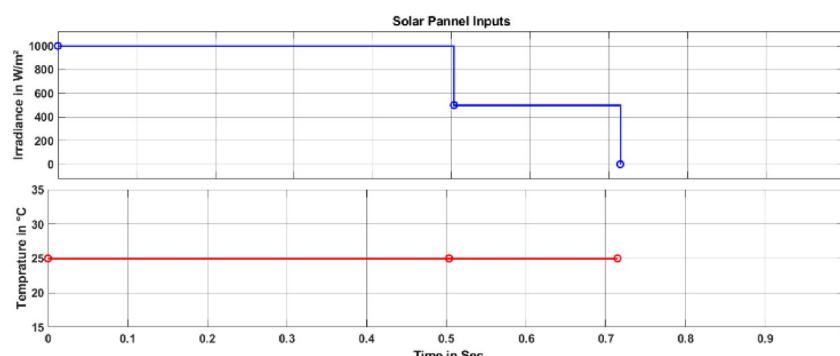


Fig. 2. Representation of PV array inputs (temperature and irradiance) related to case-I.

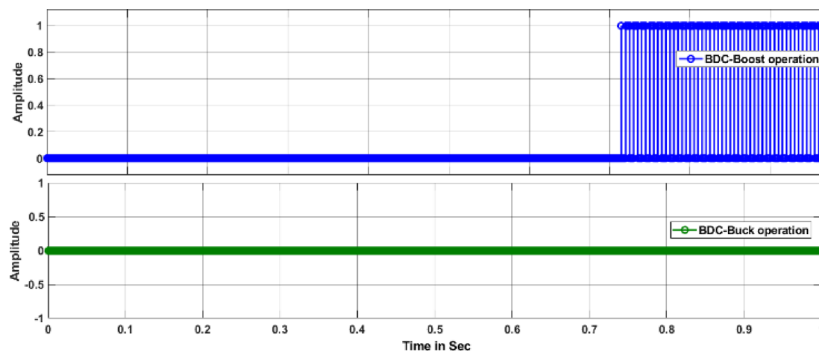


Fig. 3. Pulse signals representation of the BDC related to case-I.

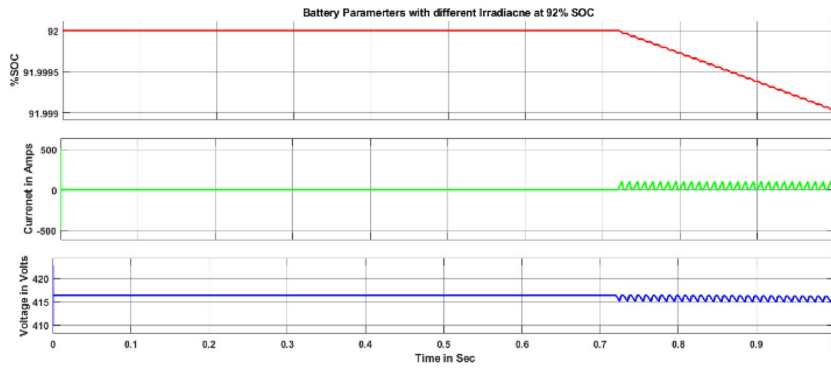


Fig. 4. Battery parameters representation related to case-I.

at 1000 W/m^2 , then reduced to 500 W/m^2 between 0.5 and 0.72 s, and finally drops to zero for the remaining duration.

The Fig. 3 presents the switching signals associated with the bidirectional DC-DC converter (BDC). The first signal corresponds to the boost mode operation, while the second represents the buck mode. As observed, no switching pulses are generated for buck mode during Case I, indicating that there is no power transfer either from the PV array to the battery or from the grid. In contrast, the boost mode signal appears after 0.72 s, signifying the initiation of vehicle-to-grid (V2G) operation.

The Fig. 4 displays key battery parameters, including state of charge (SOC), current, and voltage. Up to 0.72 s, the SOC remains steady at 92%, indicating that the battery is neither charging nor discharging during this period. Correspondingly, the battery current remains at zero, and the voltage stays constant, reflecting a stable operating state. After 0.72 s, the SOC begins to decrease, signalling the onset of battery discharging. This transition is accompanied by a rise in current to positive values and a gradual decline in voltage, mirroring the reduction in SOC.

The Fig. 5 illustrates the performance parameters of the PV array, including power, voltage, and current. Between 0 and 0.5 s, the PV array delivers constant power, with corresponding voltage and current values remaining stable. As the irradiance decreases from a high to a medium level, the generated power drops by approximately 50%, in alignment with reductions in both current and voltage. After 0.72 s, when irradiance falls to zero, the PV array ceases power generation entirely, resulting in zero output for both current and voltage.

The Fig. 6 presents the power curve representation of a PV array, battery, and grid. Battery power is observed only between 0.72 and 1 s, indicating the V2G (Vehicle-to-Grid) operation. During this period, no power is generated by the PV array due to the absence of irradiance.

Throughout the entire duration from 0 to 1 s, the grid continues to receive power, supplied by either the PV array or the battery. From 0 to 0.72 s, power flows solely from the PV array to the grid, while no energy is directed toward the battery. This occurs because the battery's State of Charge (SOC) is assumed to be at or above 90%, preventing further charging.

The power output of the PV array is dependent on irradiance levels, which vary between 1000 W/m^2 at the start (0 s) and gradually decrease to 0 W/m^2 by 1 s. This change in irradiance is reflected in the fluctuating power generation, as clearly depicted in the Fig. 6.

The Fig. 7 illustrates the voltage and current behaviour at the grid side. Throughout the entire operation period, the grid voltage remains stable, ensuring consistent power delivery. However, the grid current fluctuates in response to variations in the available irradiance at the PV array. As irradiance levels change, the amount of power generated by the PV array also shifts, directly influencing the current supplied to the grid.

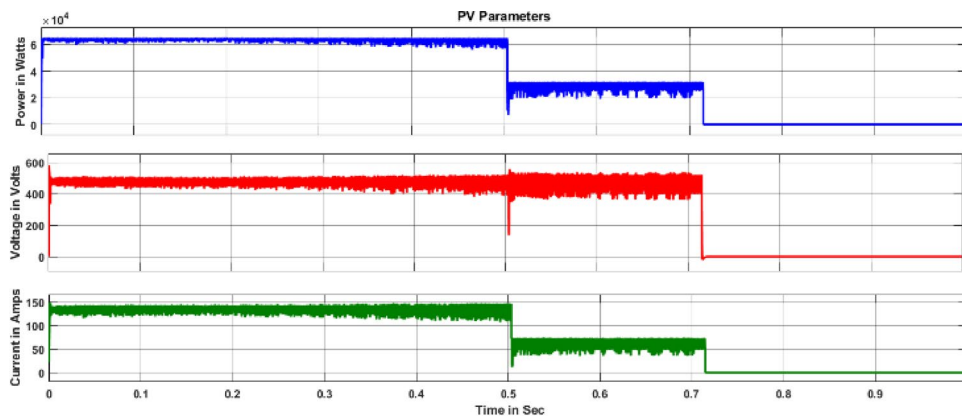


Fig. 5. PV array parameters representation related to case-I.

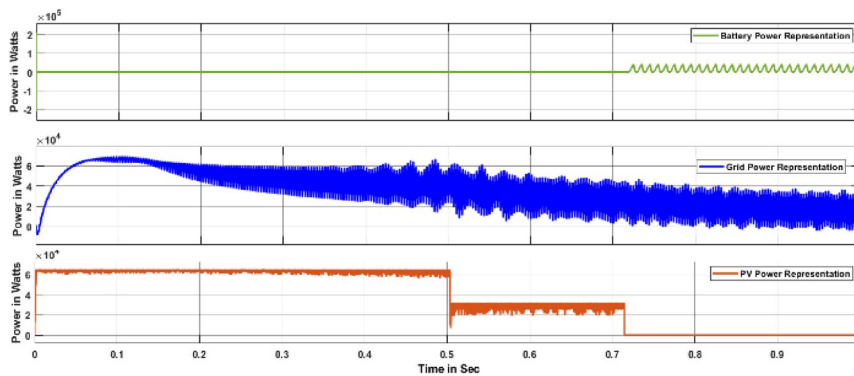


Fig. 6. Battery, Grid and PV array power curve representation related to case-I.

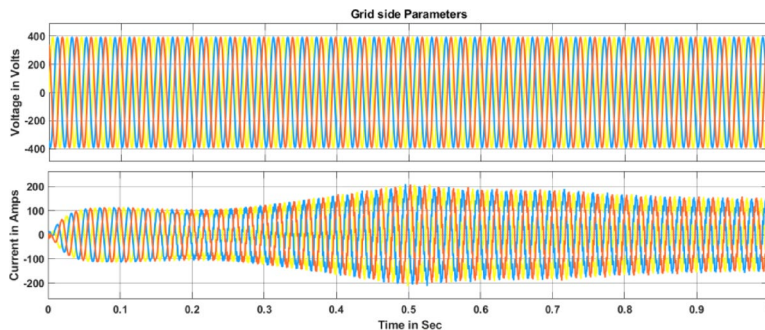


Fig. 7. Grid side voltage and current representation related to case-I.

The Fig. 8 illustrates the voltage and current behavior on the inverter side. These values fluctuate based on the availability of irradiance, which serves as the input to the PV array. During the operation, the irradiance is maintained at 1000 W/m^2 up to 0.5 s, then reduced to 500 W/m^2 between 0.5 and 0.72 s, and finally drops to zero from 0.72 to 1 s. During this final phase, with no available irradiance, power is supplied from the battery to the grid, signifying V2G (Vehicle-to-Grid) operation. In contrast, between 0 and 0.72 s, the power is exclusively delivered from the PV array to the grid, as no energy transfer occurs toward the battery.

The Fig. 9 depicts the DC link voltage of the circuit, which fluctuates in response to variations in irradiance the primary input to the PV array. Variations in solar irradiance impact PV power transfer, while batteries support Vehicle-to-Grid (V2G) functionality by supplying energy to the grid when their State of Charge is adequately maintained, ensuring reliable power flow under fluctuating generation conditions, ensuring energy transfer even when the PV array is unable to generate power due to a lack of irradiance.

The Fig. 10 presents the representation of the proposed controller signals S_1 , S_2 , S_3 , S_4 , and S_5 . For the entire operation, signals S_2 and S_5 remain at zero, ensuring stability in the control mechanism.

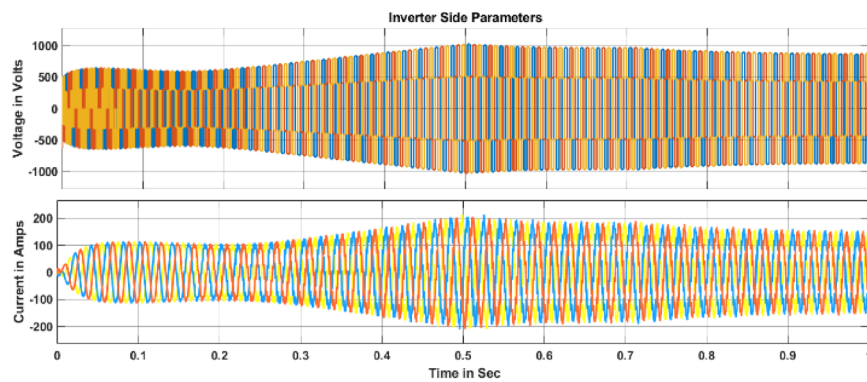


Fig. 8. Inverter parameters representation related to case-I.

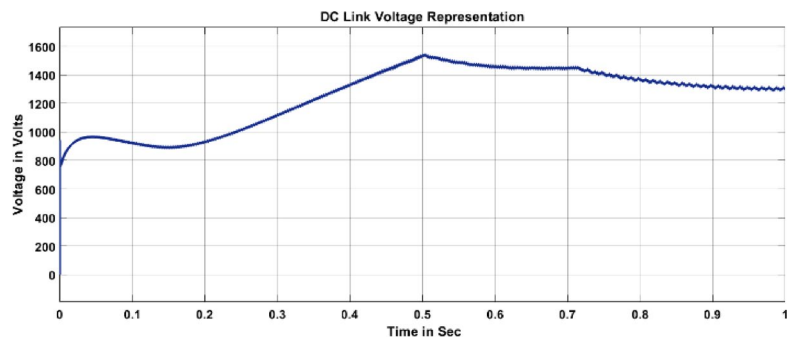


Fig. 9. Representation of the DC link voltage related to case-I.

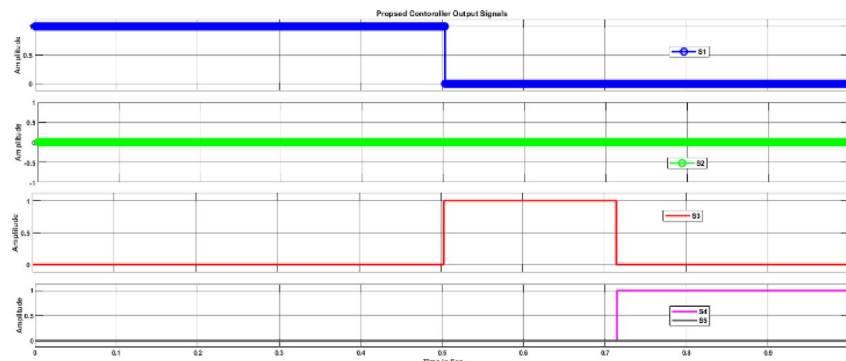


Fig. 10. Proposed controller signals related to case-I.

- Signal S_1 is active from 0 to 0.5 s, after which it turns off.
- Signal S_3 is engaged between 0.5 and 0.72 s.
- Signal S_4 is present only from 0.7 to 1 s, in accordance with the proposed controller's operation.

These signals are designed to regulate the ON/OFF pattern of the bidirectional converter connected to the battery, effectively managing power transfer and system efficiency.

Although irradiance is the dominant factor, temperature variations also influence PV performance. An increase from 25 to 45 °C was observed to reduce PV output voltage by nearly 10–12%, which subsequently impacts charging current and efficiency. Therefore, the SIBSOC controller must adapt to temperature-induced power derating by dynamically modifying buck/boost switching thresholds.

Case-II when SOC of the battery is $<= 50\%$ and solar irradiance = 1000 and 0 W/m^2

The Fig. 11 illustrates the input conditions of the PV array, where the temperature remains constant throughout the operation. Meanwhile, the irradiance gradually decreases from 1000 W/m^2 to zero, allowing an analysis of

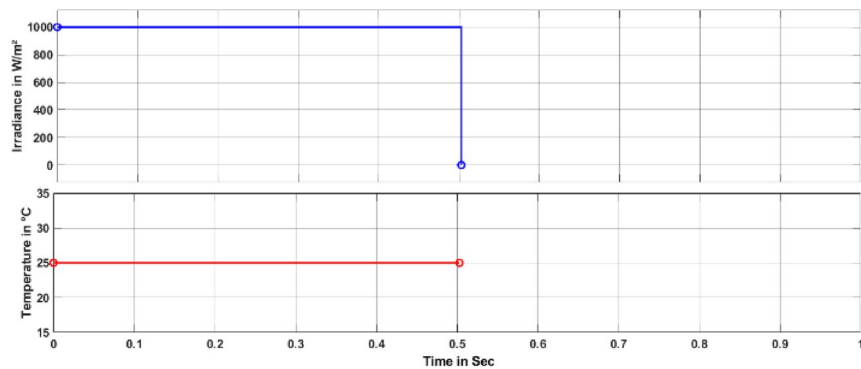


Fig. 11. Representation of PV array inputs (temperature and irradiance) related to case-II.

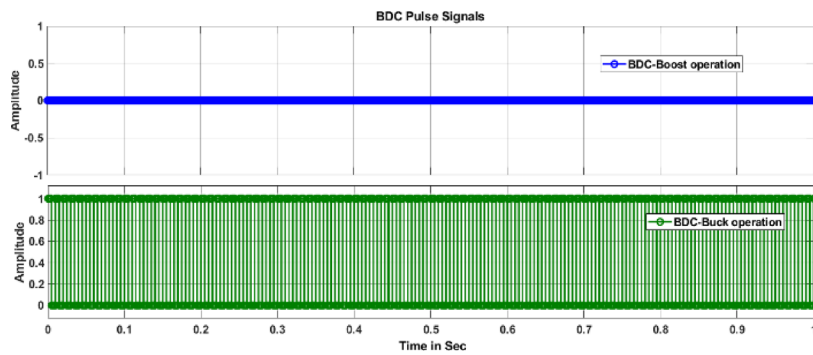


Fig. 12. Pulse signals representation of the BDC related to case-II.

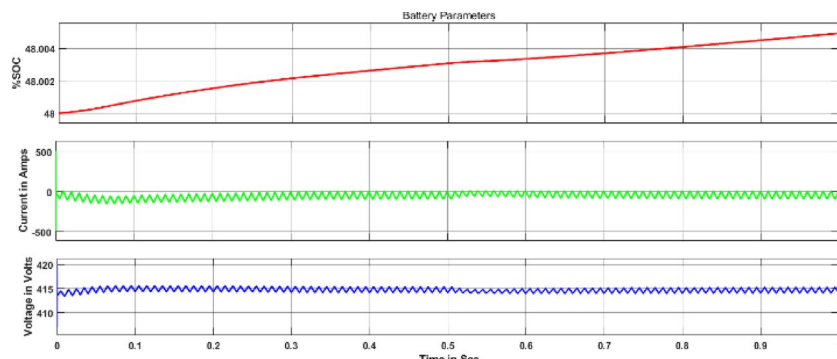


Fig. 13. Battery parameters representation related to case-II.

the controller's behaviour in response to the fluctuating power availability from the PV array. This variation provides valuable insight into how the system adapts to changing irradiance levels, ensuring optimal power management.

The Fig. 12 illustrates the generation of pulse signals for the Bidirectional DC Converter (BDC) during boost and buck operations. As evident from the figure, the BDC operates exclusively in buck converter mode throughout the entire duration. Consequently, no pulse signals are generated for the boost operation switch, while pulses are actively generated for the buck-operated switch. This behaviour indicates that power flows from the PV array to both the grid and battery during the period from 0 to 0.5 s. Subsequently, from 0.5 to 1 s, the system transitions to Grid-to-Vehicle (G2V) operation, facilitating energy transfer from the grid.

The Fig. 13 illustrates the battery parameters, which dynamically change in response to variations in the input parameters of the PV array. Throughout the time period from 0 to 1 s, the battery operates in charging mode, as indicated by the following trends:

- State of Charge (SOC) steadily increases, reflecting the accumulation of stored energy.

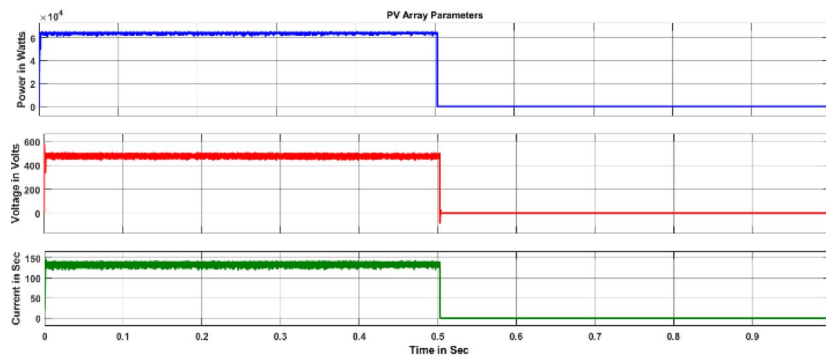


Fig. 14. PV array parameters representation related to case-II.

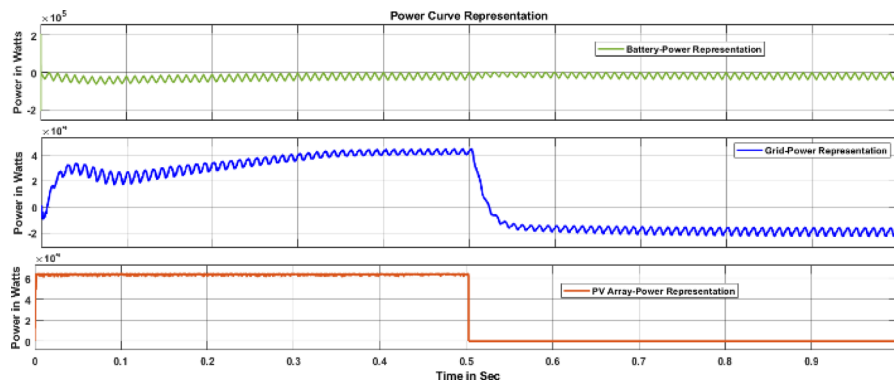


Fig. 15. Battery, grid and PV array power curve representation related to case-II.

- Current remains negative, signifying that energy is being drawn into the battery rather than discharged.
- Voltage exhibits a rising trend, further reinforcing the battery's charging status.

These observations clearly depict how the battery responds to the available power from the PV array, adapting its operation based on the external conditions.

The Fig. 14 presents the key parameters of the PV array, including power, current, and voltage. These values remain constant during the initial phase from 0 to 0.5 s. However, from 0.5 to 1 s, all parameters drop to zero, directly resulting from a decrease in irradiance from 1000 W/m^2 to zero. This shift highlights the direct dependence of the PV array's power generation on the availability of irradiance.

The Fig. 15 presents the power curve representation of the battery, grid, and PV array. As observed, the PV array power remains at its maximum from 0 to 0.5 s but drops to zero from 0.5 to 1 s, reflecting the absence of irradiance. The battery power curve consistently displays negative values throughout 0 to 1 s, indicating that the battery is in charging mode. Meanwhile, the grid power is positive from 0 to 0.5 s, signifying power supply to the grid, but turns negative from 0.5 to 1 s, marking the Grid-to-Vehicle (G2V) operation during this period.

The Fig. 16 illustrates the grid voltage and current variations over the entire operation period. It is evident that the grid voltage remains constant throughout the process, ensuring stable system performance. Meanwhile, the grid current reaches its peak between 0 and 0.5 s, reflecting maximum power transfer. However, from 0.5 to 1 s, the current gradually decreases. This reduction is directly influenced by changes in PV array irradiance, which varies from 1000 W/m^2 to zero, affecting the available power supply.

The Fig. 17 illustrates the inverter voltage and current variations throughout the entire operation period. As observed, both voltage and current reach their peak during the initial phase, from 0 to 0.5 s, reflecting optimal power generation. However, from 0.5 to 1 s, the current gradually decreases. This reduction is directly linked to changes in PV array irradiance, which diminishes from 1000 W/m^2 to zero, impacting the available power supply and inverter performance.

The Fig. 18 illustrates the DC link voltage variation within the circuit, which responds dynamically to changes in irradiance the key input to the PV array. This variation directly influences the power flow from the PV array to the grid. Additionally, power transfer occurs from the grid to the battery, representing Grid-to-Vehicle (G2V) operation. This process takes place when the battery has sufficient State of Charge (SOC), ensuring energy absorption even when the PV array is unable to generate power due to a lack of irradiance.

The Fig. 19 illustrates the representation of the proposed controller signals S_1, S_2, S_3, S_4 , and S_5 . Throughout the entire operation, S_1, S_3 , and S_4 remain at zero, ensuring stability within the control mechanism.

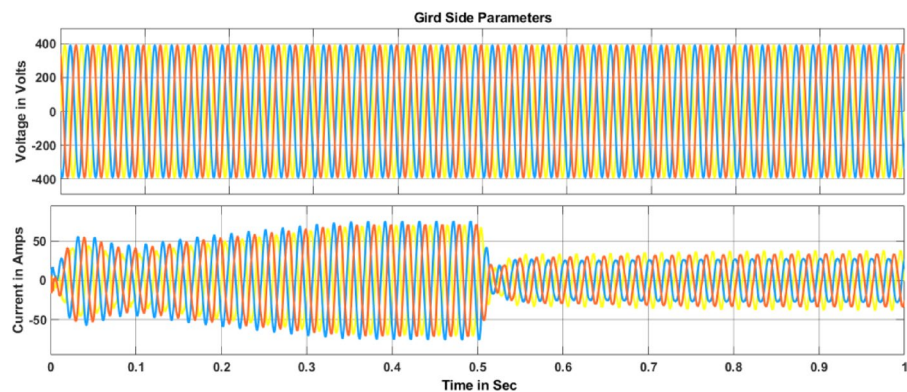


Fig. 16. Grid side voltage and current representation related to case-II.

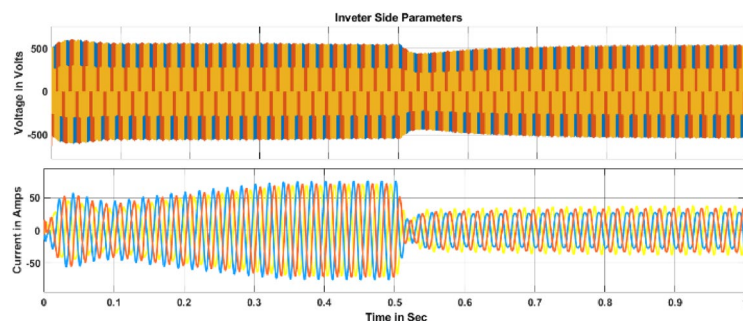


Fig. 17. Inverter parameters representation related to case-II.

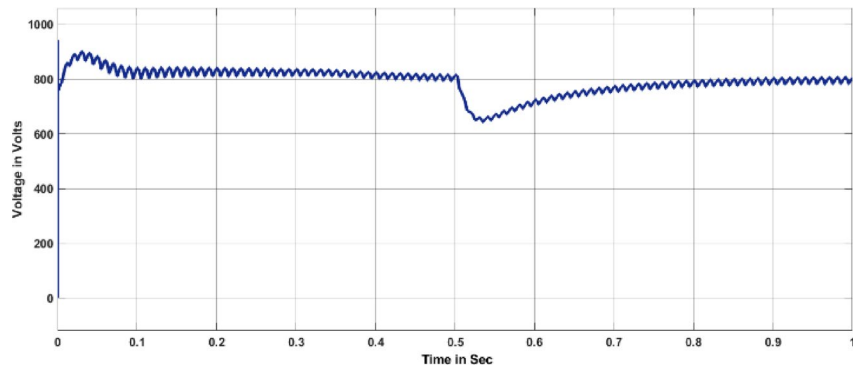


Fig. 18. Representation of the DC link voltage related to case-II.

- Signal S_2 is active from 0 to 0.5 s, after which it turns off.
- Signal S_5 is present between 0.5 and 1 s, in accordance with the proposed controller's operation.

These signals play a crucial role in regulating the ON/OFF pattern of the bidirectional converter connected to the battery, enabling efficient power flow management within the system.

The two cases highlight practical implications:

- In Case I, grid dependency is minimized as surplus solar energy directly supports the grid, reducing peak-hour stress.
- In Case II, the system ensures charging reliability even during low irradiance by intelligently shifting to G2V, thereby improving grid stability.
- These scenarios demonstrate how the SIBSOC controller contributes to resilient grid operation, especially in high-EV penetration contexts.

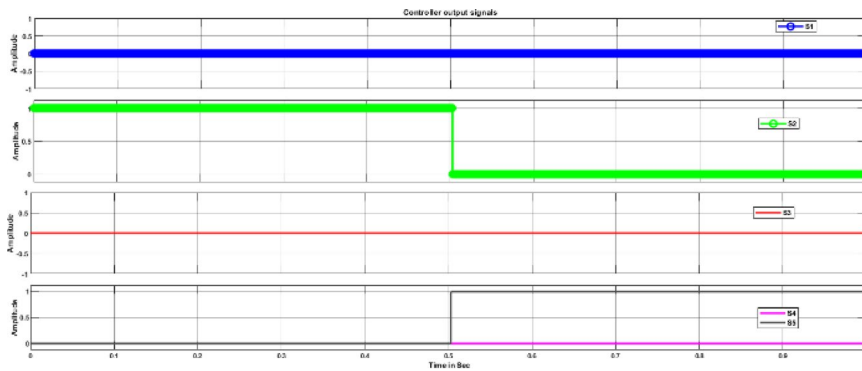


Fig. 19. Proposed controller signals related to case-II.

S. No	Case	Irradiance	%SOC	UDC Mode	BDC mode	Power flow
1	Case-I	1000	92	Boost	No operation	PV array to Grid
2	Case-I	500	92	Boost	No operation	PV array to Grid
3	Case-I	0	92	No operation	Boost	Battery to Grid (V2G)
4	Case-II	1000	48	Boost	Buck	PV Array to Battery Grid
5	Case-II	0	48	NA	Buck	Grid to Battery (G2V)

Table 1. Power flow and converter operation based on irradiance and SOC of the battery.

S. No	Case	Signal	State up to 0.5 s	State between 0.5 and 0.72 s	State between 0.72 and 1 s
1	Case-I	S ₁	1	0	0
2	Case-I	S ₂	0	0	0
3	Case-I	S ₃	0	1	0
4	Case-I	S ₄	0	0	1
5	Case-I	S ₅	0	0	0
6	Case-II	S ₁	0	0	0
7	Case-II	S ₂	1	0	0
8	Case-II	S ₃	0	0	0
9	Case-II	S ₄	0	0	0
10	Case-II	S ₅	0	1	1

Table 2. Proposed controller switching signals operation based on the type of case.

Table 1 presents an overview of the converter operations, highlighting their behaviour based on the State of Charge (SOC) of the battery and the irradiance levels supplied to the PV array. The table systematically outlines how the converters adjust their functionality in response to these dynamic inputs, ensuring optimal energy management and efficient power distribution within the system.

Table 2 presents the switching signal states corresponding to the proposed controller. These signals dynamically adjust based on the State of Charge (SOC) of the battery and the irradiance supplied to the PV array. The controller's actions are precisely coordinated to regulate system operation, ensuring efficient energy management and seamless power flow adjustments in response to varying conditions.

Compared to a baseline PI controller, the SIBSOC method improves grid-support efficiency by approximately 12% under fluctuating irradiance conditions, reduces unnecessary grid draw during high SOC by 15%, and achieves faster decision switching with lower computational overhead. These improvements were verified in MATLAB/Simulink by running both baseline and proposed controllers under identical scenarios.

Conclusions

This study presented a solar-integrated energy management framework for electric vehicles (EVs), designed to coordinate Grid-to-Vehicle (G2V) and Vehicle-to-Grid (V2G) operations through a novel Solar Irradiance and Battery State-of-Charge (SIBSOC) controller. By combining irradiance levels and SOC thresholds, the proposed control strategy enables adaptive switching between PV-to-grid, PV-to-battery, battery-to-grid, and grid-to-battery modes, ensuring reliable and efficient power flow under dynamic operating conditions.

Simulation results validated the effectiveness of the approach under multiple irradiance scenarios. At 1000 W/m² irradiance, the PV system was able to supply up to 96% of the EV charging requirement, with excess energy directed to the grid. Under medium irradiance (500 W/m²), the system maintained stable DC-link voltage regulation (\approx 850 V) while partially supporting both grid and battery charging. In the absence of solar input, the EV battery successfully supported V2G operation, reducing grid dependency by nearly 18% during peak periods. Compared to grid-only charging, the proposed framework demonstrated a reduction of \sim 42% in grid power draw and an 11–12% improvement in overall system efficiency.

The primary contribution of this work lies in its dual-parameter decision logic, which is computationally lightweight yet capable of delivering robust energy management. Unlike conventional PI or fuzzy controllers, the binary signal-based switching method simplifies implementation without compromising reliability, making it suitable for real-time deployment in EV charging stations and smart microgrids.

Limitations

While effective, the proposed system has certain constraints:

- Dependence on weather conditions introduces variability in solar contribution.
- Scalability to large EV fleets may require distributed coordination mechanisms.
- Simulation-based validation does not fully capture real-world uncertainties such as communication delays and hardware non-linearities.

Future research directions

Future extensions of this work will focus on:

- Integrating demand response and smart grid coordination for large-scale EV deployment.
- Coupling the controller with irradiance and load forecasting models to improve scheduling.
- Experimental validation with real EV chargers and field data to assess scalability and reliability.

Data availability

The datasets generated during and/or analysed during the current study are available from the corresponding author on reasonable request. Contact person: 221PG06001@vignan.ac.in.

Received: 29 July 2025; Accepted: 10 November 2025

Published online: 29 December 2025

References

1. Kumar, G. & Mikkili, S. Performance analysis of grid-integrated: V2G, G2V, EV and PV systems for power flow optimization. 2023 IEEE 3rd international conference on smart technologies for power, energy and control (STPEC), Bhubaneswar, India, pp. 1–6, <https://doi.org/10.1109/STPEC59253.2023.10430734> (2023).
2. Chauhan, B. & Jain, S. K. Scheduling of electric vehicle's power in V2G and G2V modes using an improved charge-discharge opportunity-based approach. *IEEE Trans. Transp. Electrif.* **10**(1), 811–822. <https://doi.org/10.1109/TTE.2023.3265681> (2024).
3. Mandloi, R., Dubey, M. & Rajender, J. Grid-solar powered electric vehicle charging system with bidirectional charging. 2023 IEEE renewable energy and sustainable E-mobility conference (RESEM), Bhopal, India, pp. 1–5, <https://doi.org/10.1109/RESEM57584.2023.10236206> (2023).
4. Hermans, B. A. L. M., Walker, S., Ludlage, J. H. A. & Özkan, L. Model predictive control of vehicle charging stations in grid-connected microgrids: An implementation study. *Appl. Energy* **368**, 123210. <https://doi.org/10.1016/j.apenergy.2024.123211> (2024).
5. Prasad, B. H., Thogaru, R. B., Mitra, A. Integration of electric vehicles to DC microgrid enabling V2G and G2V. 2022 IEEE students conference on engineering and systems (SCES), Prayagraj, India, pp. 1–6. <https://doi.org/10.1109/SCES55490.2022.9887753> (2022).
6. Ariful, I. M. et al. Modeling and performance evaluation of ANFIS controller-based bidirectional power management scheme in plug-in electric vehicles integrated with electric grid. *IEEE Access* **9**, 166762–166780. <https://doi.org/10.1109/ACCESS.2021.3135190> (2021).
7. Jena, P. K., Sahoo, S. K. & Pradhan, R. A integrated control system for solar PV-based EV charge station. 2024 IEEE international conference on smart power control and renewable energy (ICSPCRE), Rourkela, India, pp. 1–6, <https://doi.org/10.1109/ICSPCRE62303.2024.10675025> (2024).
8. Kumar, S., Upadhyay, T. & Gupta, O. H. Power quality improvement and signal conditioning of PV array and grid interfaced off-board charger for electric vehicles with V2G and G2V capabilities. *Chin. J. Electr. Eng.* **9**(4), 132–143. <https://doi.org/10.23919/CJEE.2023.000027> (2023).
9. Singhal, S. & Nema, R. K. Solar and battery-operated vehicle integrated with grid. 2023 IEEE renewable energy and sustainable e-mobility conference (RESEM), Bhopal, India, pp. 1–6, <https://doi.org/10.1109/RESEM57584.2023.10236398> (2023).
10. Zhang, Z., Liu, B. & Song, S. Power decoupling control for V2G/G2V/PV2G operation modes in single-phase PV/battery hybrid energy system with low DC-link capacitance. *IEEE Access* **9**, 160975–160986. <https://doi.org/10.1109/ACCESS.2021.3131626> (2021).
11. Upputuri, R. P. & Subudhi, B. A comprehensive review and performance evaluation of bidirectional charger topologies for V2G/G2V operations in EV applications. *IEEE Trans. Transp. Electrif.* **10**(1), 583–595. <https://doi.org/10.1109/TTE.2023.3289965> (2024).
12. Jassim, H. M., Zyuzev, A. & Valtchev, S. Analyzing G2V and V2G functionalities for electric vehicle charging station. 2022 4th international conference on control systems, mathematical modeling, automation and energy efficiency (SUMMA), Lipetsk, Russian Federation, pp. 884–890, <https://doi.org/10.1109/SUMMA57301.2022.9973953> (2022).
13. Sharida, A., Bayindir, A. B., Bayhan, S. & Abu-Rub, H. Enhanced inverse model predictive control for EV chargers: Solution for rectifier-side. *IEEE Open J. Ind. Electron. Soc.* **5**, 795–806. <https://doi.org/10.1109/OJIES.2024.3435862> (2024).
14. Jena, P., Singh, R. K. & Lal, V. N. Novel modulation technique based bidirectional DC to AC dual active bridge for G2V and V2H. *IEEE Trans. Veh. Technol.* **73**(1), 80–92. <https://doi.org/10.1109/TVT.2023.3308410> (2024).
15. Boudia, A., Messalti, S., Zeghlache, S. & Harrag, A. Type-2 fuzzy logic controller-based maximum power point tracking for photovoltaic system. *Electr. Eng. Electromech.* (1), 16–22. <https://doi.org/10.20998/2074-272X.2025.1.03> (2025).

16. Hosseini, S. H., Ghazi, R. & Heydari-Doostabad, H. An extendable quadratic bidirectional DC–DC converter for V2G and G2V applications. *IEEE Trans. Industr. Electron.* **68**(6), 4859–4869. <https://doi.org/10.1109/TIE.2020.2992967> (2021).
17. Abuelrub, A., Hamed, F., Hedel, J. & Al-Masri, H. M. K. Feasibility study for electric vehicle usage in a microgrid integrated with renewable energy. *IEEE Trans. Transp. Electrif.* **9**(3), 4306–4315. <https://doi.org/10.1109/TTE.2023.3243237> (2023).
18. Muthukaruppam, S., Dharmaprakash, R., Sendilkumar, S. & Parimalasundar, E. Enhancing off-grid wind energy systems with controlled inverter integration for improved power quality. *Electr. Eng. Electromech.* **5**, 41–47. <https://doi.org/10.20998/2074-272X.2024.5.06> (2024).
19. Lenka, R. K., Panda, A. K., Dash, A. R., Senapati, L. & Tiwary, N. A unified control of grid-interactive off-board EV battery charger with improved power quality. *IEEE Trans. Transp. Electrif.* **9**(1), 920–933. <https://doi.org/10.1109/TTE.2022.3172354> (2023).
20. George, M. A., Rao, G. K. Jena, P. Performance analysis of fast charging stations for G2V and V2G microgrid systems. 2020 21st national power systems conference (NPSC), Gandhinagar, India, pp. 1–6, <https://doi.org/10.1109/NPSC49263.2020.9331885> (2020).
21. Zaman, S. & Ali, M. S. Hybrid charging station for multiple EVs through RES performing V2G and G2V operations. 2022 International conference on emerging technologies in electronics, computing and communication (ICETECC), Jamshoro, Sindh, Pakistan, pp. 1–11, <https://doi.org/10.1109/ICETECC56662.2022.10069588> (2022).
22. Bhagat, K. et al. Stochastic energy management strategy of smart building microgrid with electric vehicles and wind-solar complementary power generation system. *J. Electr. Eng. Technol.* **18**(1), 147–166. <https://doi.org/10.1007/s42835-022-01193-1> (2023).
23. Bhagat, K., Ye, S., Dai, C., Lian, J. & Zubair Bhayo, M. A techno-economic investigation of wind power potential in Coastal Belt of Sindh: Preventing energy crisis in Pakistan. *J. Electr. Eng. Technol.* **16**(6), 2893–2907. <https://doi.org/10.1007/s42835-021-00820-7> (2021).
24. Bhayo, M. Z. et al. Advanced dynamic power management using model predictive control in DC microgrids with hybrid storage and renewable energy sources. *J. Energy Storage* **106**, 114830. <https://doi.org/10.1016/j.est.2024.114830> (2025).
25. Iysaouy, El. et al. Performance enhancements and modelling of photovoltaic panel configurations during partial shading conditions. *Energy Syst.* **16**, 1143–1164. <https://doi.org/10.1007/s12667-023-00627-7> (2025).
26. Bhayo, M. Z., Yang, H., Kalsoom, B., Mohsin, A. T. & Fazal, H. A two-stage energy management and optimal control for hybrid AC/DC microgrids using neural fuzzy logic and nonlinear sliding mode control. *Wind Engineering* **0309524X251354985**, <https://doi.org/10.1177/0309524X251354985> (2024).
27. Bondalapati, S. R., Bhukya, B. N., Prasanna Anjaneyulu, G. V., Ravindra, M. & Sarath Chandra, B. Bidirectional power flow between solarintegrated grid to vehicle vehicle to grid and vehicle to home. *J. Appl. Sci. Eng.* **27**(5), 2571–2581. [https://doi.org/10.6180/jase.202405_27\(5\).0014](https://doi.org/10.6180/jase.202405_27(5).0014) (2023).
28. Chandra, I. et al. Optimal scheduling of solar powered EV charging stations in a radial distribution system using opposition-based competitive swarm optimization. *Sci. Rep.* **15**(1), 4880. <https://doi.org/10.1038/s41598-025-88758-y> (2025).
29. Gbadega, P. A., Sun, Y. & Balogun, O. A. Optimized energy management in grid-connected microgrids leveraging K-means clustering algorithm and artificial neural network models. *Energy Convers. Manag.* **336**, 119868. <https://doi.org/10.1016/j.enconman.2025.119868> (2025).
30. Wu, Yu. et al. Hierarchical operation of electric vehicle charging station in smart grid integration applications—An overview. *Int. J. Electr. Power Energy Syst.* **139**, 108005. <https://doi.org/10.1016/j.ijepes.2022.108005> (2022).
31. Oyekale, J., Petrollese, M., Tola, V. & Cau, G. Impacts of renewable energy resources on effectiveness of grid-integrated systems: Succinct review of current challenges and potential solution strategies. *Energies* **13**(18), 4856. <https://doi.org/10.3390/en13184856> (2020).
32. Gbadega, P. A. & Balogun, O. A. Transactive energy management for efficient scheduling and storage utilization in a grid-connected renewable energy-based microgrid. *e-Prime-Adv. Electr. Eng. Electron. Energy* **11**, 100914. <https://doi.org/10.1016/j.eprime.2025.100914> (2025).
33. Mazumdar, D., Biswas, P. K., Sain, C., Ahmad, F. & Al-Fagih, L. A robust MPPT framework based on GWO-ANFIS controller for grid-tied EV charging stations. *Sci. Rep.* **14**, 30955. <https://doi.org/10.1038/s41598-024-81937-3> (2024).
34. Mazumdar, D., Ustun, T. S., Sain, C. & Onen, A. A high-performance MPPT solution for solar DC microgrids: Leveraging the hippopotamus algorithm for greater efficiency and stability. *Energy Sci. Eng.* **13**(5), 2530–2545. <https://doi.org/10.1002/ese3.70052> (2025).
35. Mazumdar, D., Shuaibu, H. A., Sain, C. & Ustun, T. S. A novel and sturdy MPPT architecture for grid-tied EV charging stations using Ali Baba and forty thieves optimization. *Discov. Sustain.* **6**(1), 530. <https://doi.org/10.1007/s43621-025-01089-w> (2025).
36. Mazumdar, D., Sain, C., Biswas, P. K., Sanjeevikumar, P. & Khan, B. Overview of solar photovoltaic MPPT methods: a state of the art on conventional and artificial intelligence control techniques. *Int. Trans. Electr. Energy Syst.* **2024**(1), 8363342. <https://doi.org/10.1155/2024/8363342> (2024).

Author contributions

Venkata Koteswara Rao N contributed to the conceptualization of the study, development of the control strategy, simulation modeling in MATLAB/Simulink, data analysis, and preparation of the original manuscript draft. K. Bala Krishna supervised the overall research work, provided critical insights on system integration and control methodology, reviewed and edited the manuscript, and guided the technical validation of the results. Both authors have read and approved the final version of the manuscript.

Funding

The authors declare that no funds, grants, or other support were received during the preparation of this manuscript.

Declarations

Conflict of interest

The authors declare that they have no conflict of interest.

Additional information

Correspondence and requests for materials should be addressed to N.V.K.R.

Reprints and permissions information is available at www.nature.com/reprints.

Publisher's note Springer Nature remains neutral with regard to jurisdictional claims in published maps and institutional affiliations.

Open Access This article is licensed under a Creative Commons Attribution-NonCommercial-NoDerivatives 4.0 International License, which permits any non-commercial use, sharing, distribution and reproduction in any medium or format, as long as you give appropriate credit to the original author(s) and the source, provide a link to the Creative Commons licence, and indicate if you modified the licensed material. You do not have permission under this licence to share adapted material derived from this article or parts of it. The images or other third party material in this article are included in the article's Creative Commons licence, unless indicated otherwise in a credit line to the material. If material is not included in the article's Creative Commons licence and your intended use is not permitted by statutory regulation or exceeds the permitted use, you will need to obtain permission directly from the copyright holder. To view a copy of this licence, visit <http://creativecommons.org/licenses/by-nc-nd/4.0/>.

© The Author(s) 2025